Modular Development of CAE Models for Lossy Matching Networks: Part I

Shaohua Li, Perry Wheless

***Abstract*—We consider here fundamental computer-based models for the multimode behavior of single-layer helical air-core RF inductors at frequencies up to approximately 1.5 GHz. Four specific CAE models are presented, with discussion of their merits and limitations. This study is one in a series, motivated by the desire to improve practical design and analysis of efficient antenna tuning units, power amplifier tank circuits, and other RF applications employing helical air-core RF inductors.**

***Index Terms*— Antenna tuning units, RF inductors, inductor CAE, electronic component models.**

I. Introduction

Antenna design projects often include the design of a companion antenna tuning unit (ATU) to match the transmitter and transmission line characteristic impedance to the impedance(s) presented at the antenna element feed point(s). For moderate to high operating power levels at frequencies from LF (30 - 300 kHz) up into the UHF (300 MHz - 3 GHz) region, the fundamental ATU subsystems to achieve phase and power division control are networks comprising three reactive components. RF inductors and capacitors are typically configured in Tee or Pi circuits, and radio system engineers generally are aware how they can scientifically determine three L and C values that will match an arbitrary (finite) complex load impedance Z_L to a desired real input impedance Z_0 at a specific design frequency, and simultaneously provide a desired phase shift in the process. RF power amplifiers similarly have tuned (tank) circuits involving both inductors and capacitors. ATU and amplifier tank circuit losses are always in the background consciousness of design engineers, and losses may be significant, but typical circumstance is that the designer lacks the computer-aided engineering (CAE) tools for an accurate and reliable analysis of the network losses. This article is the first in a series, which will culminate in the computer-based tools to thoroughly characterize such networks, including losses, in practical applications.

Achievement of the objective of useful CAE software is an evolutionary project which, of course, is predicated on beginning from correct fundamental principles and appropriate engineering models. The starting point, therefore, is an examination and modeling of the essential characteristics and behavior of the helical air coils and variable plate capacitors typically found in ATUs and tank circuits. This paper reports some highlight results from first studying RF inductor basics.

The authors are with the Department of Electrical and Computer Engineering, University of Alabama, Tuscaloosa, AL. E-mail: li022@bama.ua.edu.

II. Illustrative Case Study

To enable quantitative treatment of RF inductor behavior, a specific (but typical) helical air coil is discussed. To facilitate some comparisons to [1], we here adopt a coil of the same dimensions, namely, 12.9 single-layer turns of 18-gauge copper wire with the following nominal dimensions: an inside solenoid radius of $a_i = 0.248$ inches, mean radius of the solenoid $a = 0.268$ inches, axial length $c = 0.89$ inches, and pitch $\Psi = 0.041$. When the inductor is horizontally mounted above a ground plate, the S_{21} transmission characterization, as measured in manual mode by a Hewlett-Packard 8505A vector network analyzer, is shown in Figure 1. This data closely emulates that given in [1], with individual data points marked by small circles. We parenthetically note that excellent interpolation of values between the measurement points is available in MATLAB [2] by use of the *interp1* function with the 'pchip' (piecewise cubic Hermite interpolation) option. The *interp1* function was utilized in generation of the solid line plots in Figure 1.

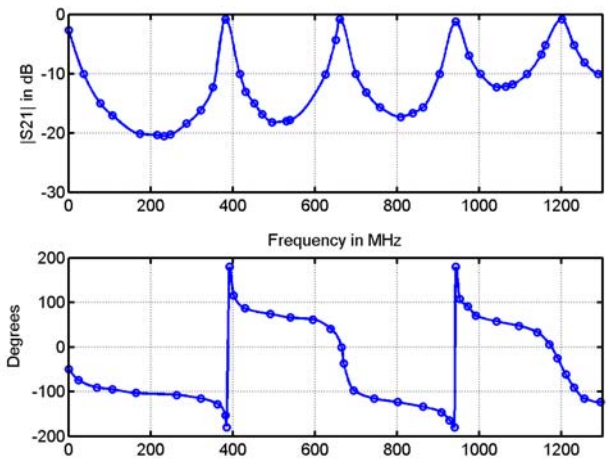

Fig. 1. S_{21} of horizontally mounted RF inductor.

Figure 1 straightaway shows a behavior pattern that may be surprising to some RF design engineers. The "classic model" for a real-world RF inductor, which is the subject of the next section, clearly indicates that, at sufficiently high frequency, the device will be self-resonant. RF circuit designers are well-aware of the reality of that resonance effect, and carefully avoid it in requirements such as, for example, an RF choke in the bias circuit of a high-power tube amplifier. The surprise, at least for some, is that real RF inductors exhibit not just one, but multiple resonances, as frequency is increased.

Experimental characterization, illustrated by Figure 1, is more useful as a guide to appropriate models for RF inductors than as a routine design aid. Engineers are inclined by their training to develop and work with models, and justifiably so, because accurate and reliable models may be used and extended to new and various circumstances, versus the rigid limitation that measured data is obtained under constrained and quite specific conditions. In short, good engineering models offer a high degree of flexibility and convenience. In the following sections, we will discuss a series of basic models that are all amenable to computer implementation as a CAE tool. Through application to the same "case study" inductor, the objective is for the reader to acquire a good sense of the relative power and limitations of each model.

III. Classic Model

The so-called "classic" model, widely depicted in undergraduate electrical engineering textbooks on circuit theory and basic electronics, is shown in Figure 2. Rhea [1] is a good reference for a summary review discussion of the classic model. From only a casual consideration of Figure 2, one can quickly and correctly conclude that this will be a low-frequency model of limited general utility, and so we restrict our discussion of the classic model here.

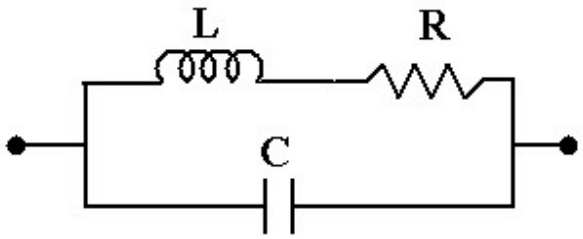

Fig. 2. Classic model of an RF inductor.

Wheeler [3] developed an almost exact low-frequency (i.e., quasi-static) classic inductor model that requires the calculation of complete elliptic integrals. An approximation formula which does not require elliptic integrals, but is accurate at low frequencies to approximately 1% for coil lengths greater than 0.67 times the radius, is

$$L = \frac{n^2 a^2}{9a + 10c} \simeq 1\ \mu H \tag{1}$$

with $n = 12.9$ T, $a = 0.268$ inch, and $c = 0.890$ inch. Medhurst [4] gives the capacitance relationship

$$C\ (\text{in pF}) = H \times D \Longrightarrow C \simeq 0.65\ \text{pF} \tag{2}$$

where $D = 2a$ (in cm) and H is a function of $\frac{c}{2a}$, the length-to-diameter ratio. Please see [4] or Table 1 of [1] for how H is obtained from $\frac{c}{2a}$.

$$\frac{c}{2a} = \frac{0.89}{2 \times 0.268} = 1.6604 \Longrightarrow H = 0.48 \tag{3}$$

The estimation of R starts with the relation for unloaded Q [4]

$$Q_u = 0.15 a \varphi \sqrt{f_0} \tag{4}$$

with f_0 in units of Hz and φ is determined from its relation to $\frac{c}{2a}$ and $\frac{d_w}{s}$ (the fraction of axial length c occupied by wire) in accordace with Table 2 of [1]. Here, $\frac{d_w}{s} = 0.58$ for 18-gauge copper wire, giving $\varphi \simeq 0.72$ and

$$Q_u = 0.15 \times (0.268 \times 0.0254) \times 0.72 \times \sqrt{f_0} \tag{5}$$

and, finally,

$$R = \frac{\omega L}{Q_u} = \frac{2\pi f_0 L}{Q_u}. \tag{6}$$

Since R is a function of frequency, it is calculated as a vector inside the MATLAB modeling program.

To enable the classic model to show its best possible predictions in comparison to the measured data, two low-frequency ranges were selected and, also, the MATLAB modeling program performed a least squares optimization of the nominal numerical values of R, L, and C via the function *lsqcurvefit* provided in the MATLAB package. The graphical result for $|S_{21}|$ for the restricted frequency range 1 to 50 MHz (in steps of 1 MHz) is in Figure 3, where it is evident that the optimized parameter values of $L = 1.0619\ \mu H$ and $C = 0.65349$ pF improve on the original model fit. The low-frequency (static) classic model is moderately successful in predicting the actual experimental data up to a frequency of 50 MHz.

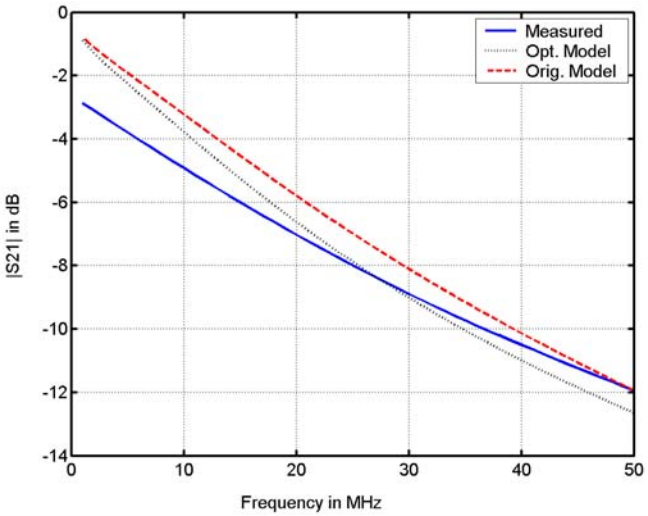

Fig. 3. Classic model vs measured, 1-50 MHz.

However, when we just extend the frequency range of interest to 1 - 300 MHz, still far from the full range of 1 - 1300 MHz, the classic model already exhibits breakdown (see Figure 4). It is immediately clear that this elementary model is not even a candidate for the multimode reality shown in Figure 1. It is visually difficult to discern if the optimized classic model is actually better than the original classic model in Figure 4, so we introduce a quantitative measure of error at this point.

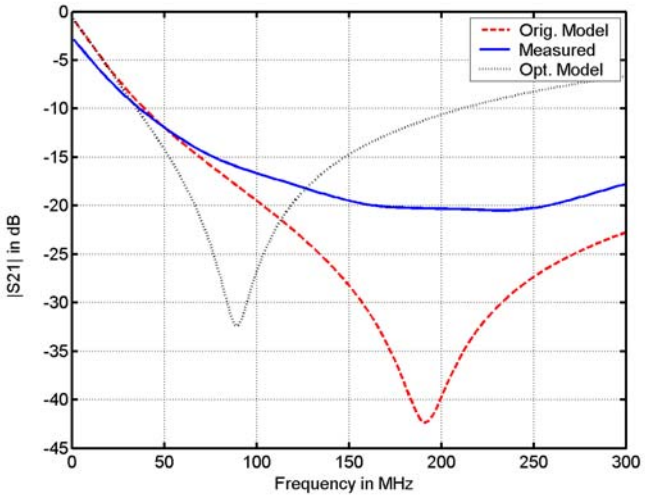

Fig. 4. Classic model vs measured, 1-300 MHz.

IV. Quantification of Model Error

In this paper, the measured data is taken as the standard reference, and the various model predictions are then compared to the experimental data. The measure of model discrepancy is then the "SSE" (sum of the errors squared). For all modeling cases reported here, the frequency step is 1 MHz. Therefore, comparing the results for two different models with 1-300 MHz results presented is direct and immediate, without the need for additional manipulation or interpretation. When the frequency span is different, some interpretation is necessary. To facilitate comparisons in those instances, the total SSE is divided by the number of points at which the composite calculation was made, yielding an SSE_{avg} value *per point*.

The observant reader will quickly note that the original measurement points depicted in Figure 1 are not in 1 MHz steps, and wish to know the procedure applied in the event a frequency for analysis does not exactly match one of the original measurement frequencies. In those cases, the standard value for model accuracy comparison is determined by interpolation between the nearest original measured data points in MATLAB using the *interp1* function with 'pchip' option, as previously discussed.

Using this error quantification technique, the 1-50 MHz classic model result of Figure 3 has a $|S_{21}|$ error of $SSE = 136.83$ ($SSE_{avg} = 2.74$ per pont) for the original component values, and $SSE = 66.92$ ($SSE_{avg} = 1.34$ per point) for the least squares optimized component values. For the 1-300 MHz classic model result of Figure 4, the original values give $SSE = 24,685$ ($SSE_{avg} = 82.3$ per point) and the optimized components yield modeling error $SSE = 22,451$.($SSE_{avg} = 74.8$ per point) Hence, the optimized classic model curve in Figure 4 really is a better fit to the measured curve than that of the original classic model.

V. Transmission Line Model

A new multimode model for the helical air-core RF inductor was proposed in 1997 in [1]. In this model, the inductor is replaced with a section of transmission line of electrical length Θ degrees and characteristic impedance Z_0, as indicated in Figure 5. In Figure 1, we note that $|S_{21}|$ has its first local minimum just above 200 MHz, and then makes its first return approach to 0 dB at approximately 383 MHz. The response at 383 MHz suggests that the appropriate transmission line length at this frequency is 180°.

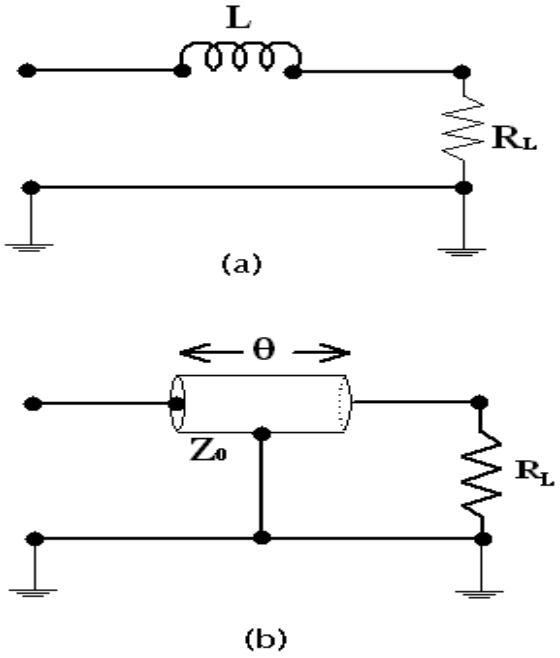

Fig. 5. Transmission line model.

A computer-aided implementation again aids our appreciation of the essential merit of this particular model. Two instructive results are included here. In both cases, the MATLAB program was allowed in each case to apply the *lsqcurvefit* function in order to optimize the values of line length and Z_0 to provide the best possible fit against the measured data. Figure 6 shows model performance from 1 to 395 MHz in 1 MHz steps:

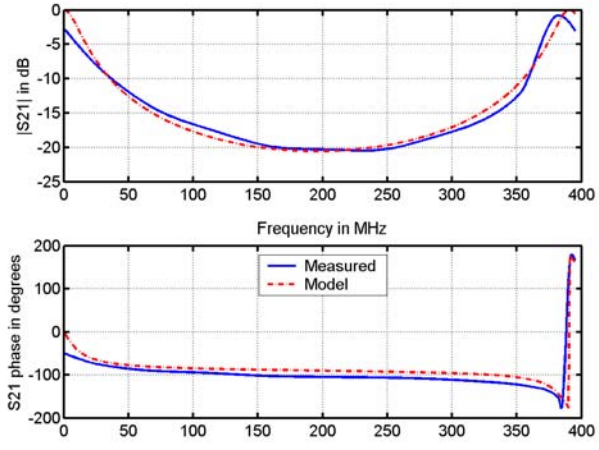

Fig. 6. Transmission line model, 1-395 MHz.

The modeling error calculations associated with Figure 6 are $SSE\ |S_{21}| = 415.5$, or $SSE_{||avg} = 1.052$ per point, and $SSE\ \measuredangle S_{21} = 2.42 \times 10^5$, or $SSE_{\measuredangle avg} = 614.5$ per point. It was deemed desirable, for illustration and comparison purposes, to capture the first inductor "resonance" in the frequency range of examination, although this choice clearly adversely affected the SSE result for the phase angle to a significant degree. For the full 1-1300 MHz range of measured data is modeled, the result is Figure 7.

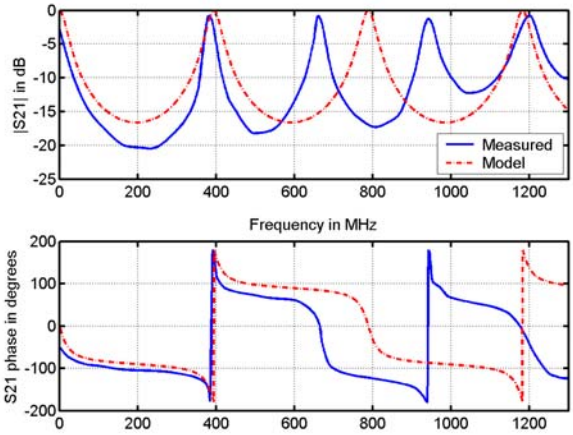

Fig. 7. Transmission line model, 1-1300 MHz.

As one would expect, the transmission line section has precisely periodic repetitions of its fundamental behavior. Figure 7 emphasizes that the higher frequency resonances of the real-world RF inductor, on the other hand, are not at integer multiples of the fundamental frequency. The modeling error calculations associated with Figure 7 are $SSE\ |S_{21}| = 48596$, or $SSE_{||avg} = 37.4$ per point, and $SSE\ \measuredangle S_{21} = 1.646 \times 10^7$, or $SSE_{\measuredangle avg} = 1.27 \times 10^4$ per point. One is led by these two results to conclude that the transmission line model can be a quite effective tool at low to medium frequencies (below the first resonance, here about 383 MHz), but its range of validity does not extend to the higher-frequency regime.

VI. Helically Conducting Sheet Model

In this section, we first present (and then extend in the next section) results using a multimode RF inductor model recently advocated by Mezak [5]. This model considers the RF inductor to be a helically conducting sheet which has both TM (transverse magnetic) and TE (transverse electric) modes and exhibits dispersion. It is especially accurate in predicting the resonant frequencies of an inductor. The key governing equations were first developed in studies on helical line models for the traveling-wave tube community in the 1960s. One of the better references for finding full details of the original derivation steps is Pierce [6]. A concise description of the calculational process, for a given frequency, follows.

First, the transcendental equation

$$(\gamma a)^2 \frac{I_0(\gamma a) K_0(\gamma a)}{I_1(\gamma a) K_1(\gamma a)} = (\beta_0 a \cot \Psi)^2 \tag{7}$$

(where $\gamma^2 = \beta^2 - \beta_0^2$, a = radius of the inductor helix, I_0 and I_1 are the modified Bessel functions of the first kind of order 0 and 1, respectively, K_0 and K_1 are the modified Bessel functions of the second kind of order 0 and 1, respectively, β_0 = propagation constant in free space, β = propagation constant of the helix, and Ψ = the helix pitch angle) is solved for γ. Then the value of β follows from the relation $\gamma^2 = \beta^2 - \beta_0^2$. The so-called transverse characteristic impedance of the helix is next found from the relation (see [6], page 30)

$$K_t = F_1 \cdot F_2 \tag{8}$$

where factor F_1 is

$$F_1 = \left(\frac{\gamma}{\beta}\right)^2 \left(\frac{\beta}{\beta_0}\right) \left[\frac{120 I_0^2}{(\gamma a)^2}\right] \tag{9}$$

and

$$F_2 = \left[\left(1 + \frac{I_0 K_1}{I_1 K_0}\right)(I_1^2 - I_0 I_2) + \left(\frac{I_0}{K_0}\right)^2 \left(1 + \frac{I_1 K_0}{I_0 K_1}\right)(K_0 K_2 - K_1^2)\right] \tag{10}$$

Choosing to use the regular chain (ABCD) matrix $\tilde{T}$ instead of the normalized chain matrix $\tilde{T}_n$, we directly take

$$Z = K_t. \tag{11}$$

Z_0 is the system characteristic impedance (typically 50Ω). Z, in turn, allows determination of the regular chain matrix elements from the well-known form for a section of transmission line

$$\begin{bmatrix} A & B \\ C & D \end{bmatrix} = \begin{bmatrix} \cos(\beta\ell) & jZ\sin(\beta\ell) \\ \frac{j}{Z}\sin(\beta\ell) & \cos(\beta\ell) \end{bmatrix} \tag{12}$$

where it should be noted that the inductor length, previously denoted c, is here denoted by ℓ. Here, the load resistor R_L in Figure 5 is equal to the system characteristic impedance Z_0, and complex S_{21} is found from

$$S_{21} = \frac{2}{A + \frac{B}{R_L} + CR_L + D}. \tag{13}$$

For short, the helically conducting sheet model will be referred to as simply the *Mezak model*. To show how the dispersion model predicts the multiple resonant frequencies rather well, the model is compared to the measured data over the full 1 - 1300 MHz range in Figure 8. On the other hand, as Figure 8 shows, this model is less successful in emulating, both qualitatively and quantitatively, the S_{21} data in between the multiple resonant frequencies.

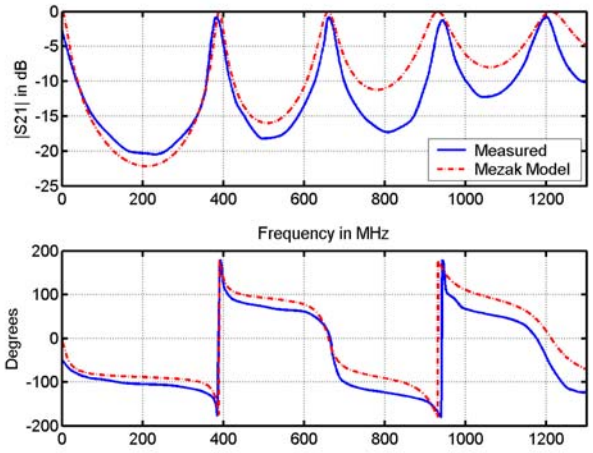

Fig. 8. Mezak model, 1 - 1300 MHz.

VII. Extended Helical Conducting Sheet Model

In applied electromagnetics, a frequent occurrence is that theoretical values for a real operational device are related to experimental measurement values through a fractional linear transformation. For example, in the context of antenna feedpoint impedances, see [7]. Motivated by favorable prior experiences, an empirical study was made of extending the so-called Mezak model to include a fractional linear transformation of the form

$$Z_m = \frac{a_1 Z_i + a_2}{a_3 Z_i + 1} \tag{14}$$

with Z_m representing measured data at a specific frequency and Z_i representing the corresponding ideal, or theoretical, value (in this case, the value from the Mezak model). The procedure for determining the complex constants a_1, a_2, and a_3 is detailed in [8]. The extended model is here called the Transformed model. A more formal name has not been chosen because the investigative study is not yet complete, and the model details remain subject to further evolutionary change.

Three results for different frequency spans are presented in Figures 9, 10, and 11 below. Data row 1 in Table I (for 1 - 200 MHz) indicates the notable extent to which the Transformed model is superior to the Mezak model in the low-frequency regime, below the first inductor resonance. Indeed, the Transformed model is the best performer in the low-frequency regime of all the models discussed in this paper. For very wide frequency ranges (see data row 3 in Table I), the Transformed model offers modest improvement over the Mezak model, although a span of 1 to 1300 MHz obviously overextends the range of validity for both.

It should be noted that there are special circumstances that result in performance degradation of the present Transformed model implementation. An example is modeling the subject RF inductor over the frequency range 1 to 395 MHz. The resonance at approximately 383 MHz actually causes the Transformed model, in its present form, to degrade the input data received from the Mezak model (see data row 2 in Table I). Work continues toward anticipating and eliminating such anomalous behavior for this model.

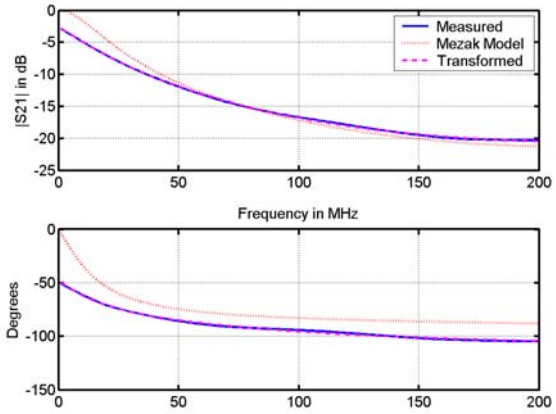

Fig. 9. Transformed model, 1-200 MHz.

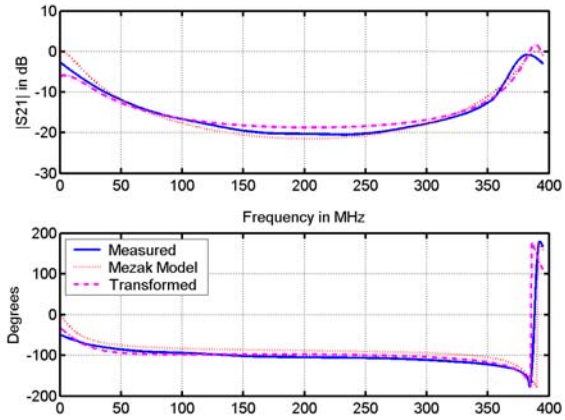

Fig. 10. Transformed model, 1- 395 MHz.

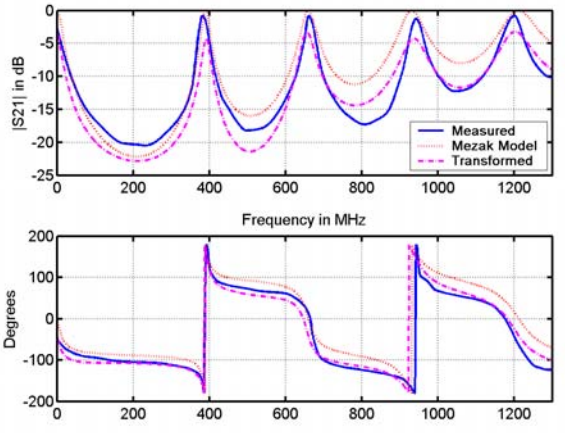

Fig. 11. Transformed model, 1 - 1300 MHz.

TABLE I
Error Comparison of Mezak and Transformed Models

Range (MHz)	Mezak $SSEs$		Transformed $SSEs$	
	$\|S_{21}\|$	$\measuredangle S_{21}$	$\|S_{21}\|$	$\measuredangle S_{21}$
1 - 200	304	5.15e4	1.94	106
1 - 395	523	2.65e5	705	2.43e5
1 - 1300	1.66e4	2.45e6	7907	2.32e6

VIII. Conclusions

Antenna engineers concerned with the design of antenna phasing and power divider networks would like computer software that provides more accurate and reliable CAE of the RF inductors and capacitors used in such practical systems. RF circuit design engineers charged with the production of high-power amplifiers share the desire of their antenna system counterparts. The ultimate objective of our work is such a computer software product, which we intend to make available in the public domain.

It is important for all radio engineers to be cognizant of the multimode behavior of real RF inductors, and aware that the widely accepted "classic model" for helical air-core coils is severely limited in its scope of applicability. Another fundamental realization of significance about RF inductors, not discussed here, is that the dominant capacitance associated RF coils is not turn-to-turn (interwinding) capacitance as long assumed, but rather the distributed capacitance with respect to ground. Reference [1] has a clear discussion of this point, and interested readers should see the *Additional Remarks* section of that paper.

This report has presented some highlight features of four RF inductor models: the classic model, the transmission line model, the so-called Mezak model, and the Transformed model incorporating a fractional linear transformation. Evidence and results examined during the course of this study first suggested that the distributed inductance and capacitance associated with inductors for RF applications made a (TEM) transmission line section a viable model candidate at sufficiently low frequencies. Later, measured inductor behavior above the first resonance of the coil then revealed that a waveguide (that is, TE/TM) model, with dispersion, becomes more appropriate at higher frequencies. The approach of [5] is based on a non-TEM, dispersive helix, and provides good predictions of inductor resonant frequencies. Because the Mezak model does not incorporate loss in its formulation, it is generally deficient in emulation of the behavior of $|S_{21}|$ and S_{21} phase away from the near neighborhoods of resonances.Work to date by the authors with the Transformed model is encouraging, and how it may accurately account for the losses associated with real-world RF inductors is being actively studied. Continuing efforts are also underway to determine if a variation of the fractional linear transformation will allow development of an even better, more comprehensive RF inductor model.

References

[1] Rhea, Randall W., "A multimode high-frequency inductor model," *Applied Microwave & Wireless*, November/December 1997, pp 70-80.

[2] MATLAB is a registered trademark of The MathWorks, Inc., 3 Apple Hill Drive, Natick, MA 01760 – 2098.

[3] Wheeler, H.A., "Inductance formulas for circular and square coils," *Proc. IEEE*, vol. 70, pp 1449-1450, 1982.

[4] Medhurst, R.G., "H.F. resistance and self-capacitance of single-layer solenoids," *Wireless Engineer*, February 1947, pp 35-43 and continued March 1947, pp 80-92.

[5] Mezak, John A., "Modeling helical air coils for wireless and RF applications," *RF Design*, January 1998, pp 77-79.

[6] Pierce, J.R., *Traveling-Wave Tubes*, New York: D. Van Nostrand Company, Inc., 1950, Chapter III and Appendix II.

[7] Kajfez, Darko and Dube, Rene L., "Measurement of impedance transformation on practical dipoles," *IEEE Trans. Antennas and Propagation*, July 1973, pp 544-549.

[8] Kajfez, Darko, "Numerical determination of two-port parameters from measured unrestricted data," *IEEE Trans. Instrumentation and Measurement*, vol. IM-24, no. 1, March 1975, pp 4-11.